# Utilization of *Mytilus* digestive gland cells for the *in vitro* screening of potential metabolic disruptors in aquatic invertebrates

Teresa Balbi, Caterina Ciacci, Elena Grasselli, Arianna Smerilli, Adriana Voci, Laura Canesi*

*Department of Earth, Environment and Life Sciences (DISTAV), University of Genoa, Corso Europa 26, 16132, Genova, Italy.*

**Running title**: Screening metabolic disruptors in mussel digestive gland cells

The ms. has 30 pages, 1 Table, 8 figures, 3 suppl. files

* Corresponding Author

Laura Canesi
DISTAV-Dipartimento di Scienze della Terra, dell'Ambiente e della Vita,
Università di Genova
Corso Europa 26
16132-Genova
Italy
Tel: +390103538259
Fax:+390103538267
Laura.Canesi@unige.it

Published in Comparative Biochemistry and Physiology, Part C on 30 August 2016, Volume 191 (2017) 26-35
https://doi.org/10.1016/j.cbpc.2016.08.009

## Abstract

In vertebrate systems, many endocrine disruptors (EDs) can also interfere with energy and lipid metabolism, thus acting as metabolic disruptors. At the cellular level, these effects are mainly mediated by interactions with nuclear receptors/transcription factors, leading to modulation of genes involved in lipid homeostasis, but also by rapid, receptor-independent pathways.
Several potential metabolic disruptors are found in aquatic environments. In fish, different EDs have been shown to affect hepatic lipid homeostasis both *in vivo* and *in vitro*. However, little information is available in aquatic invertebrates, due to our poor knowledge of the regulatory pathways of lipid metabolism.
In this work, primary cell cultures from the digestive gland of the bivalve *Mytilus galloprovincialis* were utilized to investigate the effects of model EDs (bisphenol A-BPA and perfluorooctane sulphonate-PFOS) on lipid homeostasis. Both compounds (at 24 and 3 h of exposure) increased intracellular lipid and tryglyceride-TAG content, with strongest effects of PFOS at $10^{-7}$ M. Acyl-CoA oxidase activity was unaffected, whereas some changes in the activity of glycolytic, antioxidant/ biotransformation enzymes were observed; however, no clear relationship was found with lipid accumulation. Evaluation of mitochondrial membrane potential $\Delta\psi m$ and determination of extracellular TAG content indicate that PFOS interferes with the mitochondrial function and lipid secretion, whereas BPA mainly affects lipid secretion. Experiments with specific inhibitors showed that activation of PI3-Kinase and Extracellularly Regulated Mitogen Activated Protein kinase-ERK MAPK plays a key role in mediating lipid accumulation. Mussel digestive gland cells represent a simple *in vitro* model for screening the metabolic effects of EDs in marine invertebrates.



**Key words:** cell signaling, digestive gland cells, lipid accumulation, metabolic disruptors, mussel.


## 1. Introduction

There is increasing evidence that certain environmental chemicals suspected or identified as endocrine disruptors (EDs) can also affect different metabolic pathways in mammalian systems. Several EDs (organotins, alkylphenols, phthalates, perfluorinated compounds, etc.) have been shown to induce disturbances in lipid and glucose homeostasis, this leading to the 'environmental obesogen' hypothesis (Grün and Blumberg, 2009; Grün, 2010; Heindel et al., 2015a,b). The effects can be systemic, or result from direct effects on target cells. At the cellular level, in particular in adipocytes and hepatocytes, the effects of these chemicals have been mainly ascribed to interactions with nuclear receptors/transcription factors, and modulation of expression of genes involved in lipid homeostasis (Casals-Casas and Desvergne, 2011). In addition, different EDs, including suspected obesogens, can affect kinase-mediated signal transduction, thus acting through rapid pathways independent of nuclear receptors (Masuno et al., 2005; Strack et al., 2007; Batista et al., 2012; Alonso-Magdalena et al., 2012). For example, we have previously shown that in rat FaO hepatoma cells, BPA (Bisphenol A) induced lipid accumulation acting through the phosphatidylinositol 3-kinase (PI-3K) pathway, leading to modulation of transcription of different isoforms of PPARs (Peroxisome proliferation activated receptors) and of their target genes involved in mitochondrial lipid oxidation and secretion (Grasselli et al., 2013). These results underlined the complex

interactions between different EDs and the pathways involved in lipid homeostasis in mammalian hepatic cells.

Different chemicals that represent potential metabolic disruptors are found in aquatic environments at concentrations of ng-µg/L (Hutchinson et al., 2013). In fish, disturbance in lipid homeostasis induced by tributhyltin, alkylphenols and perfluorinated compounds (PFCs) has been shown *in vivo* (Arukwe and Mortensen, 2011; Lyssimachou et al., 2015; Maradonna et al., 2015; Canesi and Fabbri, 2015; Cheng et al., 2016; Cui et al., 2016;) as well as *in vitro*, in primary hepatocytes and liver cell lines (Wågbø et al., 2012; Olufsen et al., 2014; Dimastrogiovanni et al., 2015). The results underlined changes in lipid composition and expression of genes involved in lipid homeostasis, including PPARs.

In contrast, little information is available in aquatic invertebrates, whose regulatory pathways of lipid metabolism are poorly understood. In the digestive gland of the marine bivalve *Mytilus spp.*, accumulation of neutral lipids (NL) and peroxisome proliferation (PP) have been long considered as a common response to exposure to many xenobiotics (Cajaraville, et al., 2003; Cajaraville and Ortiz-Zarragoitia, 2006). In particular, different EDs, including estrogenic compounds, pesticides and dioxins, have been shown to induce NL accumulation and affect glycolytic pathways (Canesi et al., 2007, 2008, 2011, Banni et al., 2016). However, the mechanisms underlying the metabolic effects of these chemicals in mussel digestive gland are largely unknown. In this light, the utilization of isolated digestive gland cells may represent a simple *in vitro* model for screening the direct effects of EDs on lipid homeostasis, as well as the basis for identifying their mechanisms of action. Previously, freshly isolated digestive gland cells from *M. galloprovincialis* have been proven useful for investigating the metabolic effects and intracellular signaling pathways of growth factors and heavy metals (Canesi et al., 1999, 2000, 2001).

In this work, short-term cultures (24 and 48 h post-isolation) of mussel digestive gland cells were utilized to evaluate the possible effects of known mammalian EDs on lipid accumulation in mussel cells. Primary cell cultures were first characterized for different functional parameters (lysosomal membrane stability, activities of peroxisomal, glycolytic, antioxidant and biotransformation enzymes). Cells were exposed to BPA and the results obtained were compared with previous studies in rat FaO hepatoma cells (Grasselli et al., 2013, 2014). Moreover, the effects of PFOS (perfluorooctane sulphonate) as a model of PFCs, that represent ubiquitous contaminants in coastal and estuarine environments (Kannan et al., 2005; Houde et al., 2011) were investigated.

Intracellular lipid accumulation was evaluated by ORO staining, Nile Red fluorescence, and quantification of triglyceride-TAG content. The activity of peroxisomal acyl-CoA oxidase (AOX), glycolytic enzymes (HK-hexokinase, PFK-phosphofructokinase, PK-pyruvate kinase), antioxidant (catalase) and biotransformation (GST- GSH transferase) enzymes were determined. Mitochondrial membrane potential ($\Delta\psi m$) was evaluated in order to evaluate possible disturbances in mitochondrial function. Extracellular TAG content was also determined as an indication of lipid secretion. The role of different signaling components of kinase mediated transduction pathways (PI3- Kinase and Extracellularly Regulated Mitogen Activated Protein Kinases-ERK MAPKs) in mediating chemical-induced lipid accumulation was investigated by cell pre-treatment with specific pharmacological inhibitors.

## 2. Methods

*2.1 Animals*

Mussels (*M. galloprovincialis* Lam.) 4–5 cm long, were purchased from a mussel farm in the Thyrrenian Sea (La Spezia, Italy) in May-July 2015 and kept for 1-3 days in static tanks containing synthetic sea water (1 mussel/L) at 18 C°, added with penicillin (500,000 U/L). Sea water was changed daily.

*2.2. Primary cultures of digestive gland cells*

Digestive gland cells were obtained as previously described (Canesi et al., 2000) with slight modifications. Briefly, digestive glands were collected, gently washed in calcium-magnesium-free saline buffer (CMSF; 1100 mOsm, pH 7.3, containing 20 mM HEPES, 500 mM NaCl, 12.5 mM KCl, 5 mM EDTA) and cut into pieces. Aliquots of tissue (1 g) were minced and dissociated by gentle stirring on a magnetic stirrer for 30 min at 18°C, in 25 ml of dissociating solution (0.02 % pronase w/v in CMSF). The dissociated cell suspension was filtered through a 100 μm nylon mesh, subdivided in conical Falcon plastic tubes (10 ml per tube) and centrifuged at 100 x g for 10 min at 10°C. The pellets were resuspended in 10 ml of physiological saline (PS; 1100 mOsm, pH 7.3, containing 20 mM HEPES, 436 mM NaCl, 10 mM KCl, 10 mM $CaCl_2$ and 53 mM $MgSO_4$) and again centrifuged at 100 x g for 10 min at 10 °C. The final pellets were re-suspended in 5 ml of filtered sterilized Leibovitz L-15 medium (supplemented with 350 mM NaCl, 7 mM KCl, 4 mM $CaCl_2$, 8 mM $MgSO_4$, 40 mM $MgCl_2$ and 1% pen/strep; pH 7.3). Cell suspensions obtained were maintained for 24 and 48 h at 18 °C under weak stirring, and the medium was changed every 24 hrs. Protein content was determined by the Bicinconinic method (Wiechelman et al., 1988) using bovine serum albumin (BSA) as a standard.

*2.3 Determination of functional parameters*

Lysosomal membrane stability (LMS) was evaluated in control digestive gland cells by the Neutral Red Retention Time (NRRT) assay. Aliquots of 1 mL of cell suspension (about $10^6$ cells/mL) were incubated with 5 μL of a NR solution (final concentration 40 μg/mL from a stock solution of NR 20 mg/mL in DMSO). After 15 min, 20 μL of cell suspension were pipetted onto a coverslip and observed under an optical microscope at 40 x. NRRT was evaluated as previosuly described (Canesi et al., 2008). All incubations were carried out at 18°C.

Acyl-coA oxidase (EC 1.3.3.6): Cells were homogenized in 5 vol of 20 mM Tris buffer, 0.5 M sucrose, 0,15 M NaCl, pH 7.6 and centrifuged at 500 x g for 15 min at 4 °C. Activity was measured in 500 x g supernatants. The AOX assay is based on the $H_2O_2$-dependent oxidation of dichlorofluorescein catalyzed by an exogenous peroxidase using 30 μM palmitoyl–coA as substrate (Small et al., 1985). Readings were carried out against a blank without the substrate at 502 nm at 25°C. Activity is given as mU AOX/mg protein (equivalent to nmol $H_2O_2$/min/mg protein).

Catalase (E.C. 1.11.1.6) and GSH transferase (GST) (E.C. 2.5.1.18) were evaluated as previously described (Canesi et al., 2007). Cells were homogenized as described above and centrifuged at 500 x g for 15 min at 4 °C. The supernatants were then centrifuged at 12,000 x g for 30 min. Both supernatants and pellets (containing mitochondria and peroxisomes) were utilised for evaluation of catalase activity following the decomposition of $H_2O_2$ at pH 7, 25 °C, at 240 nm. GST activity was evaluated in 12,000 x g supernatants using CDNB (1-chloro-2,4-dinitrobenzene) as a substrate. The reaction mixture (1 ml) contained 125 mM K-phosphate buffer, pH 6.5, 1 mM CDNB, 1 mM GSH.

The formation of S-2,4-dinitro phenyl glutathione conjugate was evaluated by monitoring the increase in absorbance at 340 nm.

Glycolytic enzyme activities: cells were homogenized in 5 vol of 20 mM Tris-imidazole buffer, pH 7.2, containing 10 mM EDTA (ethylenediaminetetraacetic acid), 10 mM EGTA (ethylene glycol tetraacetic acid), 0.1 PMSF (phenylmethylsulfonyl fluoride), 15 mM beta-mercaptoethanol, and centrifuged at 20,000 x g for 20 min. The supernatants were utilised for the spectrophotometric determination of HK (hexokinase, E.C. 2.7.1.1.) (Canesi et al., 1998) PFK (phosphofructokinase, E.C. 2.7.1.11) and PK (pyruvate kinase, E.C. 2.7.1.40) activities as nmoles NADH consumed/mg sample protein (Canesi et al., 2001). Data are expressed as specific activity/mg protein/ml. Spectrophotometric assays were carried out with a Varian Cary 50 spectrophotometer (Varian, Torino, Italy).

Different functional parameters were evaluated at 24 and 48 h post-isolation in 4 different cell preparations, each obtained from the digestive gland of 3-4 mussels. Since no differences were observed in different samples, data were pooled and average values are reported in Table 1 (see Results).

*2.4 Treatments*

Cells were pelleted at 100 x g and suitably suspended in L-15 supplemented medium for cell counting in a Thoma chamber. Aliquots of cell suspension (5 ml, containing about $10^6$ cells/ml) were added with BPA and PFOS from 10 mM stock solutions in methanol, suitably diluted in supplemented L-15 to obtain the desired concentrations (from $10^{-10}$ - $10^{-6}$ M). This concentration range corresponded to nominal concentrations of 50 ng/L – 500 µg/L for PFOS and 22.83 ng/l – 228.3 µg/L for BPA, respectively. Concentrations of organic chemicals in test solutions were checked by LC/MS (Supplementary File 1). Incubations were carried out for 24 h or 3 h at 18 °C. As a negative control (C), cells were incubated in the presence of vehicle alone ( ≤0.01% ethanol). As a positive control, cells were treated for 3 h with a mixture of excess free fatty acids-FFAs oleate/palmitate (2:1 molar ratio, total concentration 0.75 mM), as previously described in rat hepatoma cells (Grasselli et al., 2011, 2013). For experiments with kinase inhibitors, cell suspensions were pre-incubated for 20 min with 0.1 µM Wortmannin (Wtm) (for the PI-3K/Akt/mTor pathway), or with 20 µM PD98059 (for ERK MAPKs), suitably diluted in supplemented medium from 10 mM stock solutions in DMSO (dimethylsulfoxide) as previously described (Grasselli et al., 2013). Control samples in vehicle were run in parallel (≤0.01% DMSO). After incubation, cell suspensions were centrifuged at 100 x g for 10 min at 10°C and pellets were re-suspended in 5 ml of fresh supplemented L-15 medium. Exposure to BPA and PFOS was then carried out as described above.

*2.5 Determination of intracellular lipid content by Oil-Red-O Staining*

Neutral lipid content was evaluated using Oil-Red-O (ORO) staining. Cells were fixed with Baker's formol calcium solution [(4%, v/v) formaldehyde, 2% NaCl and 1% calcium acetate] (1 ml) for 10 min at 4°C and subsequently stained with 2.5 ml of ORO (1% w/v in 60% triethylphosphate) for 15 min in the dark. The cell suspension was centrifuged at 100 x g for 10 min at 10°C and pellets were resuspended in 2.5 ml of PS. Digital images were acquired at 40 x magnification by an Olympus BX60 light microscope equipped with a scientific grade Olympus Color ViewII CCD Camera and analysed by the Scion Image software package (Scion Corporation, Frederick, Mr, USA).

Densitometric analysis (arbitrary units/cell area in $\mu m^2$) was carried on at least 200 cells per treatment, randomly chosen from at least 10 fields. Data are reported as percent of control values.

*2.6 Determination of intra- and extracellular TAG content*

In each experimental condition, intracellular triglyceride (TAG) content was quantified in cell extracts using the commercial triglycerides liquid kit (Sentinel, Milano, Italy). After incubation, cells were briefly centrifuged and the pellet was lysed in PS passing through a 25G x 5/8'' needle syringe for 15 folds. Seventy µl of cell lysate were added with 250 µl methanol. Lipids were extracted by adding 500 µl chloroform and the resulting mixture was shaken for 1 h. After addition of 250 µl $H_2O$ and brief vortexing, samples were centrifuged at 2,000 x g for 25 min. The lower phase was collected and evaporated overnight. The dry pellet was then incubated with 500 µl of the Sentinel solution at 37˚C for 15 min. TAG content was estimated by recording the absorbance at 546 nm. Values were normalized for the protein content (mg/ml) and expressed as percent TAG content relative to controls. At the end of cell incubation, aliquots (50 µl) of extracellualar media were also collected for lipid extraction and determination of extracellular TAG content.

*2.7 Confocal Laser Scanning Microscopy (CLSM)*

Intracellular lipid accumulation was also visualized by CLSM utilizing Nile Red (NR). NR (9-diethylamino-5H-benzo [a] phenoxazine-5-one) is a phenoxazine dye used on live cells to localize and quantify neutral and polar lipids. NR stains neutral lipids yellow (emission > 528 nm) and polar lipids orange-red (emission > 590 nm) when excited at 488 nm (Greenspan et al., 1985). Aliquots of cell suspensions (50 µl), prepared as described above, were exposed for 3 or 24 hr to different concentrations of PFOS or BPA. Untreated and treated cells were incubated for 20 min with NR (1 µg/ml) before observation. When indicated, cells were also incubated for 45 minutes with 500 nM Lysotracker Green (LTG). The acidotropic dye LTG (Excitation-Emission: 504/511 nm) is freely permeant to cell membranes and typically concentrate with high selectivity in lysosomes (Canonico et al., 2014).

The mitochondrial membrane potential ($\Delta\psi m$) was evaluated by the fluorescent dye Tetramethylrhodamine ethyl ester perchlorate (TMRE) as previously described (Ciacci et al., 2012). Cells were incubated with 40 nM TMRE for 10 min before observation (Excitation-Emission: 549/574 nm). Observations were carried out by a Leica DMI 6000 CS inverted microscope (Leica Microsystems, Heidelberg, Germany) using 63 x 1.4 oil objective (HCX PL APO 63.0 x 1.40 OIL UV). Images were analyzed by the Leica Application Suite Advanced Fluorescence (LASAF) and ImageJ Software (Wayne Rasband, Bethesda, MA, USA). TMRE fluorescence intensity (arbitrary units/cell area in $\mu m^2$) in each sample was measured in at least 12 different fields. All fluorescent probes were purchased by Molecular Probes (Eugene, OR, USA).

*2.8 Statistics*

Data, representing the mean of at least 4 separate experiments in triplicate, were analysed by the one-way ANOVA plus Tukey's post-test or Mann-Whitney U test ($P<0.05$).

## 3. **Results**

*3.1 Biochemical characterization of short-term cultures of digestive gland cells*

Isolated cells, obtained from tissue samples by mild and short-time enzymatic digestion and low speed centrifugation, were kept in supplemented L-15 medium in the absence of mammalian serum for 24 and 48 h at 18°C. The cell suspension mainly contained a mixed population of digestive cells of different sizes, with larger cells filled with intracellular vacuoles, and smaller cells containing few vacuoles (Supplementary File 2a). Most of them were identified as lysosomes by Neutral Red staining (Supplementary File 2b). Few smaller cells devoid of vacuoles were also observed, probably representing basophilic cells or epithelial duct cells. Different functional parameters were determined: although slight differences were found in samples from different pools of tissues, average basal values in untreated cells did not show significant changes at 24 or 48 h of cell culture, and data from pooled samples are summarized in Table 1. High NRR times were observed (≥120 min) indicating the integrity of lysosomal membranes. Peroxisomal AOX activities were in the same range of those recorded in the tissue at the same time of the year (Cancio et al., 1999). HK, PFK, PK and catalase activities were similar those previously reported in the tissues and freshly isolated cells (Canesi at al., 1998, 1999; 2007; Birmelin et al., 1999). GST activities were comparable with those measured at tissue level and higher than those in previous studies with primary cell cultures from the digestive gland (Birmelin et al., 1999). A basal TAG content corresponding to about 3% wet weight was detected, comparable to that measured at whole tissue level (Ventrella et al., 2013). Therefore, cells cultured for 24 h were utilized for subsequent exposure experiments to different chemicals.

*3.2 Effects of BPA and PFOS on lipid accumulation*

Cells were exposed for 24 h to different concentrations of BPA and PFOS, and intracellular lipid accumulation was evaluated with different methods. BPA increased ORO staining at the highest concentration tested ($10^{-6}$ M) indicating NL accumulation; however, the results of densitometric analysis showed a large variability, with no clear dose dependent effects (not shown). When intracellular TAG content was evaluated for detection of glycerol released by triglycerides, significant increases were observed at both $10^{-7}$ and $10^{-6}$ M (+20% and +40% with respect to controls; $P<0.05$) (Figure 1). Interestingly, a comparable increase in TAG content was detected after only 3 h of exposure at $10^{-6}$ M. Lipid accumulation was also visualized in live cells by CLSM using the fluorescent lipophilic dye Nile Red. As shown in Figure 2 (upper panel), control digestive gland cells showed evident yellow fluorescence, indicating the presence of neutral lipids, and lower red fluorescence due to polar lipids. Exposure to BPA ($10^{-6}$ M, 3 h) induced a clear increase in both yellow and red fluorescence signals (Figure 2, lower panel). Similar results were obtained at 24 h (not shown).

In cells exposed to PFOS for 24 h, densitometric analysis of ORO staining clearly demonstrated a dose-dependent increase in NL accumulation, that was statistically significant from $10^{-8}$ M and maximal at $10^{-7}$ M (+67% and +200%, respectively; $P < 0.05$), with no further increases at higher concentrations (Figure 3a). Determination of intracellular TAG content showed a comparable dose-dependent increase at 24 and 3 h of exposure, with a maximal +90% increase at $10^{-7}$ M ($P < 0.05$) (Figure 3b). As a positive control, digestive gland cells were exposed for 3 h to a mixture of free fatty acids (FFAs) (oleate palmitate 2:1, final concentration 0.75 mM), as previously described in rat FaO cell lines (Grasselli et al., 2013). The FFA mixture induced a significant increase in TAG content (+40%; $P<0.05$). PFOS-induced lipid accumulation was also visualized by NR

fluorescence: an evident increase in both yellow and red fluorescence with respect to control cells was observed at $10^{-7}$ and $10^{-6}$ M (3 h) (Figure 4). The NR signal did not co-localize with that of Lysotracker green.

*3.3 Effects on enzyme activities*

The effects of PFOS and BPA, at the concentrations that induced maximal lipid accumulation ($10^{-7}$ and $10^{-6}$ M, respectively, 24 h) on the activity of different enzymes involved in peroxisomal function, antioxidant and biotransformation response, and glycolytic pathways were evaluated, and the results are reported in Figure 5. As shown in Figure 5a, neither compound affected AOX activity. Only PFOS significantly stimulated both Catalase and GST activities.(+60 and +41%, respectively; $P<0.05$).

PFOS and BPA did not affect the activity of the key glycolytic enzymes HK and PK (Figure 5b), whereas a significant stimulation of PFK was observed with PFOS (+26%; $P<0.05$). Similar results were obtained at 3 h of exposure for all enzyme activities (not shown).

*3.4 Effects on mitochondrial membrane potential*

The possible effects of PFOS and BPA on mitochondrial function were investigated by evaluating changes in membrane potential ($\Delta\psi m$) by the fluorescent dye TMRE, that exclusively stains the mitochondria and is not retained in cells upon collapse of the $\Delta\psi m$ and the results are reported in Figure 6. Representative confocal images show a strong punctuated red fluorescence in control cells (upper panel), that was clearly reduced after exposure to PFOS ($10^{-7}$ M, 3 h), indicating a decrease in $\Delta\psi m$ (lower panel) (Figure 6a). As shown in Figure 4, but better appreciated in Figure 6, PFOS did not affect lysosomal integrity, evaluated as LTG fluorescence. Quantification of the TMRE fluorescence signal indicated that PFOS ($10^{-7}$ M) induced significant decrease with respect to controls ($P<0.01$) whereas BPA was ineffective (Figure 6b).

*3.5 Effects on extracellular lipid content*

Finally, the TAG content was measured in the extracellular medium of digestive gland cells exposed for 3 h to PFOS ($10^{-7}$ and $10^{-6}$ M) and BPA ($10^{-6}$ M), respectively, as an indication of lipid secretion. A significant decrease in extracellular TAG content with respect to controls was observed in all exposure conditions (about -40%; $P<0.05$) (Figure 7).

*3.6 Possible signaling pathways involved in mediating PFOS- and BPA- induced lipid accumulation*

The possible signal transduction pathways involved in mediating contaminant-induced lipid accumulation was evaluated in cells pre-incubated with the specific inhibitors of different kinases, Wtm (for PI-3K/Akt/mTor), and PD98059 (for ERK MAPKs) and then exposed for 24 h to either PFOS or BPA (at $10^{-7}$ and $10^{-6}$ M, respectively) and the results are reported in Figure 8. Wtm reduced the increase in intracellular TAG content induced by PFOS, whereas the effect was fully prevented by PD98059. Similar results were obtained at 3 h of exposure for both TAG accumulation (not shown) and NR fluorescence (Supplementary File 3). Both inhibitors prevented the TAG accumulation induced by BPA.

## 4. Discussion

In analogy with mammalian systems, cell cultures from aquatic organisms can represent a valuable tool for studying the direct effects and mechanisms of action of environmental chemicals at the cellular level, allowing for subtle control of the experimental environment without the complex physiological conditions of *in vivo* approaches. In bivalves, the digestive gland, a tissue that plays a key role in metabolism, has been long utilized in *in vivo* studies for determination of several biomarker responses to exposure to a variety of chemicals. Primary cell cultures from digestive glands of different molluscan species have been established, with high cell viability over days/weeks (Yoshino et al., 2013). However, their experimental use has been limited by the absence of information on the maintenance of the biochemical and physiological functions of digestive cells, the most abundant cell type in the tissue, that are crucial in determining the effects and mode of action of contaminants, i.e. those related to lysosomal, biotransformation, antioxidant and peroxisomal responses. For example, cell cultures from *Mytilus edulis* digestive gland indicated severe cellular damage of digestive cells, and loss of antioxidant and biotransformation activities as soon as 24 h post-isolation (Birmelin et al., 1999). Moreover, in isolated digestive cells, no data are available on lysosomal membrane stability, one of the most utilized biomarker of stress at the tissue level. Overall, the results indicate that, in our experimental conditions, short-term primary cultures of digestive cells retained the main functional parameters of the whole tissue, and thus they could be suitably utilized to investigate the possible effects of different EDs.

Digestive cells were exposed to the model compounds (BPA and PFOS) in a concentration range from $10^{-10}$ to $10^{-6}$ M, generally lower than those utilized in studies on lipid and glucose metabolism in mammalian cells (Grasselli et al., 2013; Watkins et al., 2015; Xu et al., 2016) and in fish hepatocytes and hepatic cell lines (Wågbø et al., 2012; Olufsen et al., 2014; Dimastrogiovanni et al., 2015). The results show that in mussel digestive gland cells both PFOS and BPA induced intracellular lipid accumulation, evaluated by different methods. A comparable increase was observed at 24 h and 3 h of exposure, indicating rapid and persistent effects. NR fluorescence did not co-localize with that of LTG, indicating that lipids were accumulated within lipid droplets and not in the lysosomal compartment. PFOS showed the strongest effects on NL accumulation, with highest effects at $10^{-7}$ M.
The effects of BPA were similar to those previously observed in rat FaO hepatoma cells after 24 h of exposure (Grasselli et al., 2013). Interestingly, the brominated BPA derivative tetrabromobisphenol A (TBBPA), as previously observed in FaO cells (Grasselli et al., 2014), did not induce lipid accumulation in digestive gland cells (not shown). In contrast, in FaO cells, no effects were observed with PFOS at concentrations up to 1x $10^{-6}$ M (Grasselli, personal communication). Actually, most data on the *in vitro* effects of PFOS on lipid metabolism in mammalian cells were obtained in adipocytes, after prolonged exposure (days/weeks), at high µicroMolar concentrations. In 3T3-L1 adipocytes, PFOS increased TAG content and altered expression of genes associated with differentiation and lipid metabolism (Watkins et al., 2015); enhanced hormone-induced differentiation, adipogenic gene expression and insulin-stimulated glucose uptake were also observed (Xu et al., 2016). The results of the present work indicate that mussel digestive gland cells are particularly sensitive to the impact of PFOS on lipid homeostasis, since significant increases in intracellular lipid content were recorded at lower concentrations and much shorter times of exposure.

Lipid accumulation in mussel digestive gland cells may be due to increased lipid synthesis, reduced secretion and oxidation. However, scattered information is available on identification of genes involved in lipid homeostasis in bivalves (Bilbao et al., 2009; Zhang et al., 2014; Dai et al. 2015). In trout RTL-W1 cells, selected EDs, including BPA, induced TAG accumulation and increased the expression of lipogenic genes (Dimastrogiovanni et al., 2015). In digestive gland cells exposed to excess FFAs, employing an experimental protocol utilized to obtain fatty rat hepatocytes, the increase in intracellular TAGs was smaller than those induced by BPA and PFOS, and much smaller than that observed in rat cells (Grasselli et al., 2011, 2013). Although these data indicate the capacity of digestive gland cells for the rapid *de novo* synthesis of TAGs from exogenous FFAs, this would not appear as the main mechanism involved in the effect of PFOS and BPA. Moreover, neither compound significantly affected the activity of fatty acid synthase (FAS) (data not shown).

PFOS and BPA may interfere with lipid β-oxidation. Digestive gland cells showed an high activity of AOX, the rate limiting enzyme in the peroxisomal β-oxidation of long chain FAs. However, neither compound affected AOX activity, as previously described in FaO cells exposed to BPA, where lipid accumulation was mainly related to downregulation of genes involved in mitochondrial lipid oxidation (Grasselli et al., 2013). In rat liver mitochondria, both BPA and PFOS have been shown to directly inhibit state 3 respiration (Nakagawa and Tayama, 2000; Wallace at al., 2013). Similarly, in mussel digestive gland mitochondria, the obesogen TBT impaired state 3 respiration (Nesci et al., 2011). Our data, showing that PFOS, but not BPA, induced a decrease in mitochondrial $\Delta\psi m$, represent a first indication that PFOS can interfere with the mitochondrial function in live digestive gland cells. Further studies are needed to investigate whether PFOS-induced lipid accumulation is specifically related to decreased mitochondrial oxidation.

Finally, PFOS and BPA may affect lipid secretion, as observed in vertebrate liver. In BALB/c mice, PFOS-induced liver lipid accumulation was associated with reduced levels of serum lipid and lipoprotein (Wang et al., 2014). In the zebrafish, PFOS affected lipid biosynthesis, fatty acid β-oxidation and excretion of VLDL/LDL lipoproteins (Cheng et al., 2016). In rat FaO cells, BPA impaired lipid secretion, as shown by decreased expression of ApolipoproteinB (apoB) and extracellular TAG content (Grasselli et al., 2013). In mussel digestive gland cells, exposure to PFOS and BPA resulted in a similar decrease in TAG content in the extracellular medium. For BPA, such a decrease paralleled the increase in intracellular TAGs, suggesting that a reduction in lipid secretion may represent the main effect of this compound on lipid homeostasis. In contrast, the greatest increase in lipid accumulation induced by PFOS was only partly justified by a decrease in secretion. In this light, interference with mitochondrial oxidation may play a role in the action of PFOS.

In order to investigate the possible effects of PFOS and BPA on glucose metabolism, the activities of key glycolytic enzymes (HK, PFK and PK) were evaluated. However, no effects were observed, except for a small stimulation only of PFK induced by PFOS. Moreover, PFOS induced significant increases in both Catalase and GST activities, whereas BPA only stimulated GST activity. Overall, the results do not indicate a relationship between the capacity of PFOS or BPA to induce lipid accumulation and changes in glycolysis or oxidative stress conditions.

In mussels, the digestive gland is the first part of the body to receive the food and it plays a central role in metabolism. Digestive cells are responsible for intracellular digestion of food particles and in nutrient distribution to reproductive tissues during gamete maturation, although the mechanisms are

still largely unknown (Dimitriadis et al., 2004 and refs. quoted therein). In particular, the digestive gland is considered as a lipid storage organ. Changes in lipid content and composition are thought to be very fast, depending on changes in the amount and types of food, as well as of physiological factors (age, reproduction), and environmental stress conditions (Ventrella et al., 2013). This capacity may require rapid mechanisms to regulate lipid metabolism. Accordingly, in digestive gland cells, the increases in lipid accumulation observed *in vitro* after BPA and PFOS treatments in different experimental conditions were extremely rapid. The possible mechanisms involved were investigated by means of specific kinase inhibitors of PI3-K and ERK MAPKs, signaling components that are involved in mediating the response to different types of extracellular signals in mussel cells (Canesi et al., 1999, 2001). The results indicate that lipid accumulation induced by both PFOS and BPA was prevented by inhibition of ERK MAPKs. Moreover Wtm, an inhibitor of the PI-3K/Akt/mTor pathway, that plays fundamental roles in regulating lipid biosynthesis and metabolism (Caron et al., 2015), significantly reduced the effects of PFOS and prevented those of BPA, as previously observed in FaO cells (Grasselli et al., 2013). Wtm also prevented lipid accumulation induced by the FFA mixture (not shown). The results indicate that activation of the PI-3K/Akt/mTor pathway may represent a significant target for potential disruptors of lipid homeostasis in invertebrate cells.

*In vivo* data are available on the effects of prolonged exposure (days) to PFOS and BPA, at µg/L concentrations, in different bivalve species, measured by different biomarker responses in different cells and tissues (Canesi et al., 2005, 2007; Fernández-Sanjuan et. al, 2013; Liu et al., 2014). The results obtained in this work indicate that *in vitro* treatment of digestive gland cells to different chemicals, in the same concentration range utilized for *in vivo* studies, is able to detect changes in lipid accumulation and in different enzymatic biomarkers at much shorter exposure times. Although in the aquatic environment different EDs, including PFOS and BPA, are estimated at much lower concentrations (ng/L) (Qi et al., 2011; Canesi and Fabbri, 2015), the results indicate the suitability of our *in vitro* model to efficiently screen the metabolic effects of different chemicals and to investigate their Mode Of Action (MOA) in mussel digestive gland. Data obtained with PFOS, a predominant species of PFC in the environment and biota (Houde et al., 2011; Qi et al., 2011), including bivalves (Kannan et al., 2002, 2005; Fernández-Sanjuan et al., 2010), address lipid homeostasis as a sensitive target for this compound. Comparison of different PNECs (Predicted No Effect Concentrations) of PFOS in aquatic organisms underlined large differences in sensitivity of invertebrate species, that are probably due to its multiple MOAs (Qi et al., 2011). Interestingly, in aquatic invertebrates, a similar scenario has been described for BPA (Canesi and Fabbri, 2015). In fish liver cell models, different EDs have been shown to induce quali- and quantitative changes in lipid and fatty acid profiles, as well as in expression of genes involved in lipid homeostasis (Wågbø et al., 2012; Olufsen et al., 2014; Dimastrogiovanni et al., 2015). However, due to the complex MOAs of each compound, no clear association between expression of lipid related genes and changes in different lipid classes has been detected. Our study merely assessed neutral lipid accumulation and not the changes in lipid composition. In this light, the observation that NR fluorescence indicated also increases in polar lipids deserves further investigation.

To date, the only available data on the effects of EDs on lipid homeostasis in invertebrates are those obtained in the freshwater model *Daphnia magna*, showing that obesogen TBT alters the transfer of

storage lipids to eggs, promoting their accumulation inside lipid droplets in post-spawning females, with the possible involvement of nuclear receptors for ecdysone, juvenile hormone and retinoids (Jordão et al. 2015). Other chemicals, including BPA, were shown to affect lipid storage as well as growth and/or reproduction responses (Jordão et al., 2016). Although the molecular targets of mammalian obesogens in invertebrates are not the same as in mammalian systems, the results suggest that different emerging contaminants can act as metabolic disruptors in an ecological context.

## 5. Conclusions

The results of the present work demonstrate the ability of PFOS and BPA to induce rapid lipid accumulation in mussel digestive gland cells through activation of kinase transduction pathways. The effects of BPA may be mainly related to decreased lipid secretion, whereas PFOS may interfere with both secretion and mitochondrial oxidation. Although the results obtained *in vitro* do not obviously imply that the same effects occur *in vivo*, primary cultures of mussel digestive gland cells can be utilized as a rapid and simple tool for screening the potential metabolic effects of environmental chemicals in marine invertebrates.

**Competing interest.** The authors declare that they have no competing interests.

**Author contributions**. TB, CC, EG and AS performed all experiments and data analyses and drafted parts of the manuscript. LC conceived the study. LC and TB wrote the ms. AV supervised the ms. All authors read and approved the manuscript.

**Acknowledgments.** This work was partially supported by Progetto di Ricerca di Ateneo (PRA) 2014, University of Genoa, prot. 10022 DISTAV.

## References

Alonso-Magdalena, P., Ropero, A.B., Soriano, S., Garcia-Arevalo, M., Ripoll, C., Fuentes, E., Quesada, I., Nadal, A., 2012. Bisphenol-A acts as a potent estrogen via non-classical estrogen triggered pathways. Mol. Cell. Endocrinol. 355, 201-207.

Arukwe, A., Mortensen, A.S., 2011. Lipid peroxidation and oxidative stress responses of salmon fed a diet containing perfluorooctane sulfonic- or perfluorooctane carboxylic acids. Comp. Biochem. Physiol. C Toxicol. Pharmacol. 154, 288-295.

Banni, M., Sforzini, S., Balbi, T., Corsi, I., Viarengo, A., Canesi, L., 2016. Combined effects of n-$TiO_2$ and 2,3,7,8-TCDD in *Mytilus galloprovincialis* digestive gland: a transcriptomic and immunohistochemical study. Environ. Res. 145, 135-144.

Batista, T.M., Alonso-Magdalena, P., Vieira, E., Amaral, M.E., Cederroth, C.R., Nef, S., Quesada, I., Carneiro, E.M., Nadal, A., 2012. Short-term treatment with bisphenol-A leads to metabolic abnormalities in adult male mice. PLoS One 7, e33814.

Bilbao, E., Cajaraville, M.P., Cancio, I., 2009. Cloning and expression pattern of peroxisomal beta-oxidation genes palmitoyl-CoA oxidase, multifunctional protein and 3-ketoacyl-CoA

thiolase in mussel *Mytilus galloprovincialis* and thicklip grey mullet *Chelon labrosus*. Gene 443, 132-142.
Birmelin, C., Pipe, R.K., Goldfarb, P.S., Livingstone, D.R., 1999. Primary cell-culture of the digestive gland of the marine mussel *Mytilus edulis* : a time-course study of antioxidant- and biotransformation-enzyme activity and ultrastructural changes. Mar. Biol. 135, 65-75.
Cancio, I., Ibabe, A., Cajaraville, M.P., 1999. Seasonal variation of peroxisomal enzyme activities and peroxisomal structure in mussels *Mytilus galloprovincialis* and its relationship with the lipid content. Comp. Biochem. Physiol. C Pharmacol. Toxicol. Endocrinol. 123, 135-144.
Canesi, L., Ciacci, C., Piccoli, G., Stocchi, V., Viarengo, A., Gallo, G., 1998. *In vitro* and *in vivo* effects of heavy metals on mussel digestive gland hexokinase activity: the role of glutathione. Comp. Biochem. Physiol. C Pharmacol. Toxicol. Endocrinol. 120, 261-268.
Canesi, L., Ciacci, C., Betti, M., Malatesta, M., Gazzanelli, G., Gallo, G., 1999. Growth factors stimulate the activity of key glycolytic enzymes in isolated digestive gland cells from mussels (*Mytilus galloprovincialis* Lam.) through tyrosine kinase mediated signal transduction. Gen. Comp. Endocrinol. 116, 241-248.
Canesi, L., Malatesta, M., Battistelli, S., Ciacci, C., Gallo, G., Gazzanelli, G., 2000. Immunoelectron microscope analysis of epidermal growth factor receptor (EGFR) in isolated *Mytilus galloprovincialis* (Lam.) digestive gland cells: evidence for ligand-induced changes in EGFR intracellular distribution. J. Exp. Zool. 286, 690-698.
Canesi, L., Betti, M., Ciacci, C., Gallo, G., 2001. Insulin-like effect of zinc in *Mytilus* digestive gland cells: modulation of tyrosine kinase-mediated cell signaling. Gen. Comp. Endocrinol. 122, 60-66.
Canesi, L., Betti, M., Lorusso, L.C., Ciacci, C., Gallo, G., 2005. '*In vivo*' effects of Bisphenol A in *Mytilus* hemocytes: modulation of kinase-mediated signalling pathways. Aquat. Toxicol. 71, 73-84.
Canesi, L., Borghi, C., Ciacci, C., Fabbri, R., Vergani, L., Gallo, G., 2007. Bisphenol-A alters gene expression and functional parameters in molluscan hepatopancreas. Mol. Cell. Endocrinol. 276, 36-44.
Canesi, L., Borghi, C., Ciacci, C., Fabbri, R., Lorusso, L.C., Vergani, L., Marcomini, A., Pojana, G., 2008. Short-term effects of environmentally relevant concentrations of EDC mixtures on *Mytilus galloprovincialis* digestive gland. Aquat. Toxicol. 87, 272-279.
Canesi, L., Negri, A., Barmo, C., Banni, M., Gallo, G., Viarengo, A., Dondero, F., 2011. The organophosphate Chlorpyrifos interferes with the responses to 17β-estradiol in the digestive gland of the marine mussel *Mytilus galloprovincialis*. PLoS One 6, e19803.
Canesi, L., Fabbri, E., 2015. Environmental effects of BPA: Focus on aquatic species. Dose Response 13, 1559325815598304.
Canonico, B., Campana, R., Luchetti, F., Arcangeletti, M., Betti, M., Cesarini, E., Ciacci, C., Vittoria, E., Galli, L., Papa, S., Baffone, W., 2014. *Campylobacter jejuni* cell lysates differently target mitochondria and lysosomes on HeLa cells. Apoptosis 19, 1225-1242.
Cajaraville, M.P., Cancio, I., Ibabe, A., Orbea, A., 2003. Peroxisome proliferation as a biomarker in environmental pollution assessment. Microsc. Res. Tech. 61, 191-202.
Cajaraville, M.P., Ortiz-Zarragoitia, M., 2006. Specificity of the peroxisome proliferation response in mussels exposed to environmental pollutants. Aquat. Toxicol. 78 Suppl 1, S117-123.

555 Caron, A., Richard, D., Laplante, M., 2015. The roles of mTOR complexes in lipid metabolism.
556 Annu. Rev. Nutr. 35, 321-348.
557 Casals-Casas, C., Desvergne, B., 2011. Endocrine disruptors: from endocrine to metabolic
558 disruption. Annu. Rev. Physiol. 73, 135-162.
559 Ciacci, C., Canonico, B., Bilaniĉovă, D., Fabbri, R., Cortese, K., Gallo, G., Marcomini, A., Pojana,
560 G., Canesi, L., 2012. Immunomodulation by different types of N-oxides in the hemocytes of
561 the marine bivalve *Mytilus galloprovincialis*. PLoS One 7, e36937.
562 Cheng, J., Lv, S., Nie, S., Liu, J., Tong, S., Kang, N., Xiao, Y., Dong, Q., Huang, C., Yang, D.,
563 2016. Chronic perfluorooctane sulfonate (PFOS) exposure induces hepatic steatosis in
564 zebrafish. Aquat. Toxicol. 176, 45-52.
565 Cui, Y., Lv, S., Liu, J., Nie, S., Chen, J., Dong, Q., Huang, C., Yang, D., 2016. Chronic
566 perfluorooctanesulfonic acid exposure disrupts lipid metabolism in zebrafish. Hum. Exp.
567 Toxicol. pii: 0960327116646615.
568 Dai, P., Huan, P., Wang, H., Lu, X., Liu, B., 2015. Characterization of a long-chain fatty acid-CoA
569 ligase 1 gene and association between its SNPs and growth traits in the clam *Meretrix*
570 *meretrix*. Gene 566, 194-200.
571 Dimastrogiovanni, G., Córdoba, M., Navarro, I., Jáuregui, O., Porte, C., 2015. Alteration of cellular
572 lipids and lipid metabolism markers in RTL-W1 cells exposed to model endocrine
573 disrupters. Aquat. Toxicol. 165, 277-285.
574 Dimitriadis, V.K., Domouhtsidou, G.P., Cajaraville, M.P., 2004. Cytochemical and histochemical
575 aspects of the digestive gland cells of the mussel *Mytilus galloprovincialis* (L.) in relation to
576 function. J. Mol. Histol. 35, 501-509.
577 Fernández-Sanjuan, M., Meyer, J., Damásio, J., Faria, M., Barata, C., Lacorte, S., 2010. Screening
578 of perfluorinated chemicals (PFCs) in various aquatic organisms. Anal. Bioanal. Chem. 398,
579 1447-1456.
580 Fernández-Sanjuan, M., Faria, M., Lacorte, S., Barata, C., 2013. Bioaccumulation and effects of
581 perfluorinated compounds (PFCs) in zebra mussels (*Dreissena polymorpha*). Environ. Sci.
582 Pollut. Res. Int. 20, 2661-2669.
583 Grasselli, E., Voci, A., Canesi, L., Goglia, F., Ravera, S., Panfoli, I., Gallo, G., Vergani, L., 2011.
584 Non-receptor-mediated actions are responsible for the lipid-lowering effects of
585 iodothyronines in FaO rat hepatoma cells. J. Endocrinol. 210, 59-69.
586 Grasselli, E., Cortese, K., Voci, A., Vergani, L., Fabbri, R., Barmo, C., Gallo, G., Canesi, L., 2013.
587 Direct effects of Bisphenol A on lipid homeostasis in rat hepatoma cells. Chemosphere. 91,
588 1123-1129.
589 Grasselli, E., Cortese, K., Fabbri, R., Smerilli, A., Vergani, L., Voci, A., Gallo, G., Canesi, L.,
590 2014. Thyromimetic actions of tetrabromobisphenol A (TBBPA) in steatotic FaO rat
591 hepatoma cells. Chemosphere 112, 511-518.
592 Greenspan, P., Mayer, E.P., Fowler, S.D., 1985. Nile red: a selective fluorescent stain for
593 intracellular lipid droplets. J. Cell. Biol. 100, 965-973.
594 Grün, F., Blumberg, B., 2009. Endocrine disrupters as obesogens. Mol. Cell. Endocrinol. 304, 19-
595 29.
596 Grün, F., 2010. Obesogens. Curr. Opin. Endocrinol. Diabetes Obes. 17, 453-459.
597 Heindel, J.J., Newbold, R., Schug, T.T., 2015a. Endocrine disruptors and obesity. Nat. Rev.
598 Endocrinol. 11, 653-661.

599 Heindel, J.J., vom Saal, F.S., Blumberg, B., Bovolin, P., Calamandrei, G., Ceresini, G., Cohn, B.A.,
600 Fabbri, E., Gioiosa, L., Kassotis, C., Legler, J., La Merrill, M., Rizzir, L., Machtinger, R.,
601 Mantovani, A., Mendez, M.A., Montanini, L., Molteni, L., Nagel, S.C., Parmigiani, S.,
602 Panzica, G., Paterlini, S., Pomatto, V., Ruzzin, J., Sartor, G., Schug, T.T., Street, M.E.,
603 Suvorov, A., Volpi, R., Zoeller, R.T., Palanza, P., 2015b. Parma consensus statement on
604 metabolic disruptors. Environ. Health. 14, 54.
605 Houde, M., De Silva, A.O., Muir, D.C., Letcher, R.J., 2011. Monitoring of perfluorinated
606 compounds in aquatic biota: an updated review. Environ. Sci. Technol. 45, 7962-7973.
607 Hutchinson, T.H., Lyons, B.P., Thain, J.E., Law, R.J., 2013. Evaluating legacy contaminants and
608 emerging chemicals in marine environments using adverse outcome pathways and biological
609 effects-directed analysis. Mar. Pollut. Bull. 74, 517-525.
610 Jordão, R., Casas, J., Fabrias, G., Campos, B., Piña, B., Lemos, M.F., Soares, A.M., Tauler, R.,
611 Barata, C., 2015. Obesogens beyond Vertebrates: lipid perturbation by Tributyltin in the
612 crustacean *Daphnia magna*. Environ. Health Perspect. 123, 813-819.
613 Jordão, R., Garreta, E., Campos, B., Lemos, M.F., Soares, A.M., Tauler, R., Barata, C., 2016.
614 Compounds altering fat storage in *Daphnia magna*. Sci. Total. Environ. 545-546, 127-136.
615 Kannan, K., Hansen, K.J., Wade, T.L., Giesy, J.P., 2002. Perfluorooctane sulfonate in oysters,
616 *Crassostrea virginica*, from the Gulf of Mexico and the Chesapeake Bay, USA. Arch.
617 Environ. Contam. Toxicol. 42, 313-318.
618 Kannan, K., Tao, L., Sinclair, E., Pastva, S.D., Jude, D.J., Giesy, J.P., 2005. Perfluorinated
619 compounds in aquatic organisms at various trophic levels in a Great Lakes food chain. Arch.
620 Environ. Contam. Toxicol. 48, 559-566.
621 Liu, C., Gin, K.Y., Chang, V.W., 2014. Multi-biomarker responses in green mussels exposed to
622 PFCs: effects at molecular, cellular, and physiological levels. Environ. Sci. Pollut. Res. Int.
623 21, 2785-2794.
624 Lyssimachou, A., Santos, J.G., André, A., Soares, J., Lima, D., Guimarães, L., Almeida, C.M.,
625 Teixeira, C., Castro, L.F., Santos, M.M., 2015. The mammalian "obesogen" Tributyltin
626 targets hepatic triglyceride accumulation and the transcriptional regulation of lipid
627 metabolism in the liver and brain of Zebrafish. PLoS One 10, e0143911.
628 Maradonna, F., Nozzi, V., Santangeli, S., Traversi, I., Gallo, P., Fattore, E., Mita, D.G., Mandich,
629 A., Carnevali, O., 2015. Xenobiotic-contaminated diets affect hepatic lipid metabolism:
630 implications for liver steatosis in *Sparus aurata* juveniles. Aquat. Toxicol. 167, 257-264.
631 Masuno, H., Iwanami, J., Kidani, T., Sakayama, K., Honda, K., 2005. Bisphenol A accelerates
632 terminal differentiation of 3T3-L1 cells into adipocytes through the phosphatidylinositol 3-
633 kinase pathway. Toxicol. Sci. 84, 319-327.
634 Nakagawa, Y., Tayama, S., 2000. Metabolism and cytotoxicity of bisphenol A and other bisphenols
635 in isolated rat hepatocytes. Arch. Toxicol. 74, 99-105.
636 Nesci, S., Ventrella, V., Trombetti, F., Pirini, M., Pagliarani, A., 2011. Tributyltin (TBT) and
637 mitochondrial respiration in mussel digestive gland. Toxicol. In Vitro 25, 951-959.
638 Olufsen, M., Cangialosi, M.V., Arukwe, A., 2014. Modulation of membrane lipid composition and
639 homeostasis in salmon hepatocytes exposed to hypoxia and perfluorooctane sulfonamide,
640 given singly or in combination. PLoS One 9, e102485.
641 Qi, P., Wang, Y., Mu, J., Wang, J., 2011. Aquatic predicted no-effect-concentration derivation for
642 perfluorooctane sulfonic acid. Environ. Toxicol. Chem. 30, 836-842.

Small, G.M., Burdett, K., Connock, M.G., 1985. A sensitive spectrophotometric assay for peroxisomal acyl-CoA oxidase. Biochem. J., 227, 205-210.

Strack, S., Detzel, T., Wahl, M., Kuch, B., Krug, H.F., 2007. Cytotoxicity of TBBPA and effects on proliferation, cell cycle and MAPK pathways in mammalian cells. Chemosphere 67, S405-S411.

Ventrella, V., Pagliarani, A., Nesci, S., Trombetti, F., Pirini, M., 2013. Dietary enhancement of selected fatty acid biosynthesis in the digestive gland of *Mytilus galloprovincialis* Lmk. J. Agric. Food Chem. 61, 973-981.

Wågbø, A.M., Cangialosi, M.V., Cicero, N., Letcher, R.J., Arukwe, A., 2012. Perfluorooctane sulfonamide-mediated modulation of hepatocellular lipid homeostasis and oxidative stress responses in Atlantic salmon hepatocytes. Chem. Res. Toxicol. 25, 1253-1264.

Wallace, K.B., Kissling, G.E., Melnick, R.L., Blystone, C.R., 2013. Structure-activity relationships for perfluoroalkane-induced *in vitro* interference with rat liver mitochondrial respiration. Toxicol. Lett. 222, 257-264.

Wang, L., Wang, Y., Liang, Y., Li, J., Liu, Y., Zhang, J., Zhang, A., Fu, J., Jiang, G., 2014. PFOS induced lipid metabolism disturbances in BALB/c mice through inhibition of low densitylipoproteins excretion. Sci. Rep. 4, 4582.

Watkins, A.M., Wood, C.R., Lin, M.T., Abbott, B.D., 2015. The effects of perfluorinated chemicals on adipocyte differentiation *in vitro*. Mol. Cell. Endocrinol. 400, 90-101.

Wiechelman, K.J., Braun, R.D., Fitzpatrick, J.D., 1988. Investigation of the bicinchoninic acid protein assay: identification of the groups responsible for color formation. Anal. Biochem. 175, 231-237.

Zhang, Y., Wang, Q., Ji, Y., Zhang, Q., Wu, H., Xie, J., Zhao, J., 2014. Identification and mRNA expression of two 17β-hydroxysteroid dehydrogenase genes in the marine mussel *Mytilus galloprovincialis* following exposure to endocrine disrupting chemicals. Environ. Toxicol. Pharmacol. 37, 1243-1255.

Xu, J., Shimpi, P., Armstrong, L., Salter, D., Slitt, A.L., 2016. PFOS induces adipogenesis and glucose uptake in association with activation of Nrf2 signaling pathway. Toxicol. Appl. Pharmacol. 290, 21-30.

Yoshino, T.P., Bickham, U., Bayne, C.J., 2013. Molluscan cells in culture: primary cell cultures and cell lines. Can. J. Zool. 1, 91(6).

## Legends

**Figure 1. Effects of BPA on intracellular triglyceride (TAG) accumulation in isolated mussel digestive gland cells.** Cells were exposed for 24 h to different concentrations of BPA ($10^{-9}$ -$10^{-6}$ M) or for 3 h to $10^{-6}$ M BPA. Data, expressed as percentage of control values, represent the mean±SD of 4 experiments in triplicate. * = $P<0.05$, ANOVA plus Tukey's post-test.

**Figure 2. Effects of BPA on Nile Red-NR fluorescence evaluated by confocal microscopy in live digestive gland cells.** Yellow: neutral lipids (Exc. 488 nm; Em: > 528 nm); Red: polar lipids (Exc. 488 nm; Em: > 590 nm). Merge: superposition of Yellow and Red signals.
Upper panel: control cells.

Lower panel: cells exposed for 3 h to $10^{-6}$ M BPA.

**Figure 3. Effects of PFOS ($10^{-10}$ -$10^{-6}$ M) on lipid accumulation isolated mussel digestive gland cells.**
a) Densitometric analysis of ORO staining in cells exposed to different concentrations of PFOS for 24 h. Data represent mean absorbance values (integrated density)/cell area). Insets report representative images of ORO staining.
b) Intracellular TAG content in cells exposed to different concentrations of PFOS for 24 h or 3 h. As a positive control, the effects of exposure for 3 h to a FFA mixture are reported.
All data, expressed as percentage of control values, represent the mean±SD of 4 experiments in triplicate. * = P<0.05, ANOVA plus Tukey's post-test.

**Figure 4. Effects of PFOS on Nile Red-NR fluorescence evaluated by CLSM in live digestive gland cells.** From left to right : representative images of NR yellow and red fluorescence as in Figure 2. Lysotracker Green fluorescence - LTG green: (Exc. 504 nm; Em. 511nm). Merge: superposition of Yellow, Red and Green signals.
Upper panel: control cells.
Middle panel: cells exposed for 3 h to $10^{-7}$ M PFOS.
Lower panel: cells exposed for 3 h to $10^{-6}$ M PFOS.

**Figure 5. Effects of BPA and PFOS on enzyme activities.** Cells were exposed for 24 h to $10^{-6}$ M BPA and $10^{-7}$ M PFOS and enzyme activities were evaluated as described in Methods. a) Acyl-coA-Oxidase (AOX), Catalase (CAT) and Glutathione transferase (GST). b) Hexokinase (HK), Phosphofructokinase (PFK) and PK (Pyruvate kinase). Data, reported as percent specific activities with respect to controls, are the mean ± SD of at least four experiments in triplicate. * = P<0.05, ANOVA plus Tukey's post-test.

**Figure 6. Effects of PFOS and BPA on TMRE fluorescence in live digestive gland cells.**
a) representative confocal images of cells exposed to PFOS (3 h, $10^{-7}$ M). Red: TMRE fluorescence; Green: Lysotracker fluorescence is also reported. Merge: superposition of red and Green signals.
b) Quantification of the TMRE fluorescence signal in cells exposed to for 3 h PFOS ($10^{-7}$ and $10^{-6}$ M) and BPA ($10^{-6}$ M). Data, expressed as % integrated fluorescence density/cell area with respect to control, are mean±SD of 4 experiments. * = P<0.05, Mann-Whitney U test.

**Figure 7. Effects of PFOS and BPA on extracellular TAG content.** Cells were exposed for 3 h to PFOS ($10^{-7}$ and $10^{-6}$ M) and BPA ($10^{-6}$ M) and TAG content vas evaluated in the extracellular medium. Data, representing the mean±SD of 4 experiments, are expressed as µg TAG/mg protein/ml. * = P<0.05, ANOVA plus Tukey's post-test.

**Figure 8. Effects of cell pretreatment with different kinase inhibitors on BPA and PFOS-induced TAG accumulation.** Cells were pre-treated with Wtm (for PI-3K/Akt/mTor) or PD98059 (for ERK MAPKs) and then exposed for 24 h to $10^{-7}$ M PFOS or $10^{-6}$ M BPA. Data, expressed as percent TAG content with respect to controls, are the mean ± SD of at least four experiments in

triplicate. * = P<0.05, all treatments *vs* control; # = P<0.05, Wtm/PFOS *vs* PFOS alone. ANOVA plus Tukey's post-test.

**Legends to Supplementary Files**

**Supplementary File 1**. **Measured concentrations of organic chemicals in exposure medium (0.1 µg /L) as determined by SPE-HPLC/MS/MS.** LOD = Limit of Detection.

**Supplementary File 2. Representative images of primary cultures (48 h) of mussel digestive gland cells by optical microscopy.** a) Control cells showing an heterogeneous cell population, with larger cells rich in intracellular vacuoles and smaller cells with fewer vacuoles. b) Neutral Red loaded cells, indicating the presence of intact lysosomes.

**Supplementary File 3. Effects of cell pretreatment with different kinase inhibitors on PFOS-induced lipid accumulation.** Confocal images of Nile Red-NR and Lysotracker Green-LTG fluorescence as in Figure 4. C: control cells. PFOS: cells exposed for 3 h to 10-7 M PFOS. Wtm/PFOS: cells pretreated with Wortmannin and exposed for 3 h to 10-7 M PFOS. PD/PFOS: cells pretreated with PD98059 and exposed for 3 h to 10-7 M PFOS.

**Fig. 1**

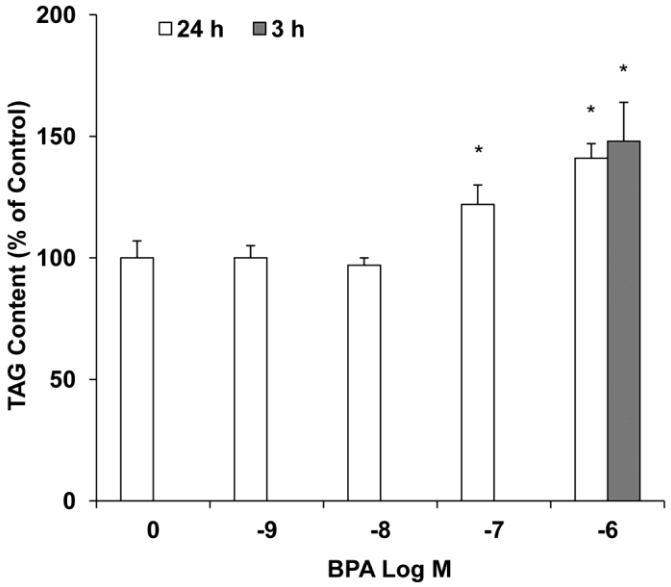

**Fig. 2**

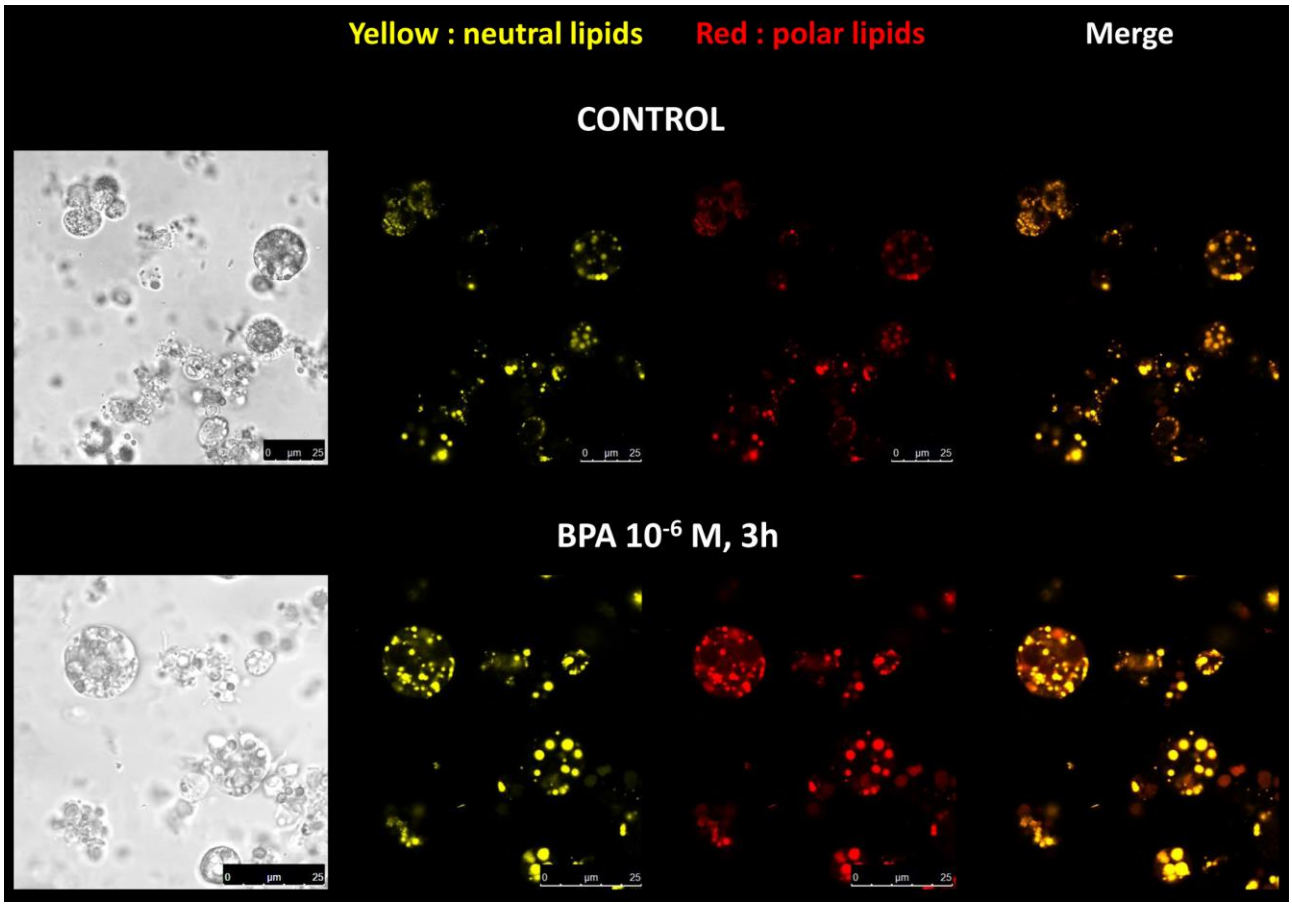
Yellow : neutral lipids
Red : polar lipids
Merge
CONTROL
BPA 10-6 M, 3h

**Fig. 3**

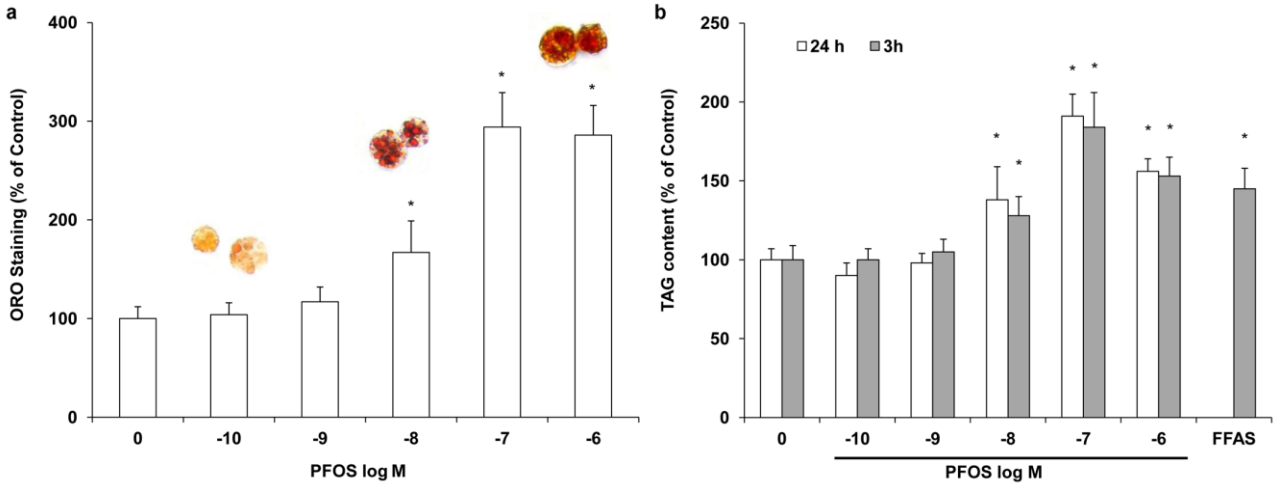
a
ORO Staining (% of Control)
400
300
200
100
0
0
-10
-9
-8
-7
-6
PFOS log M
b
TAG content (% of Control)
250
200
150
100
50
0
24 h
3h
0
-10
-9
-8
-7
-6
FFAS
PFOS log M

**Fig. 4**

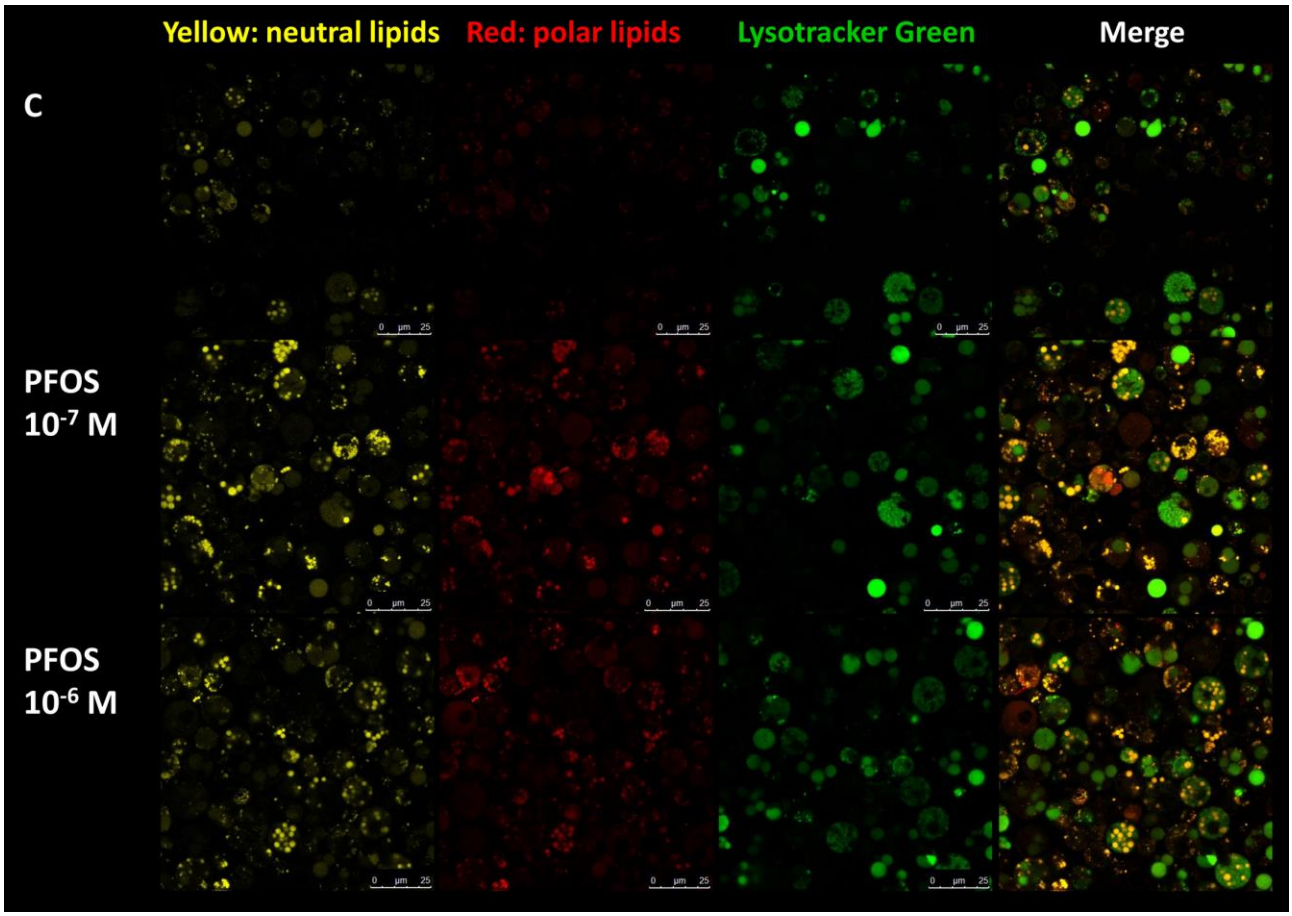
Yellow: neutral lipids
Red: polar lipids
Lysotracker Green
Merge
C
PFOS
10-7 M
PFOS
10-6 M

**Fig. 5**

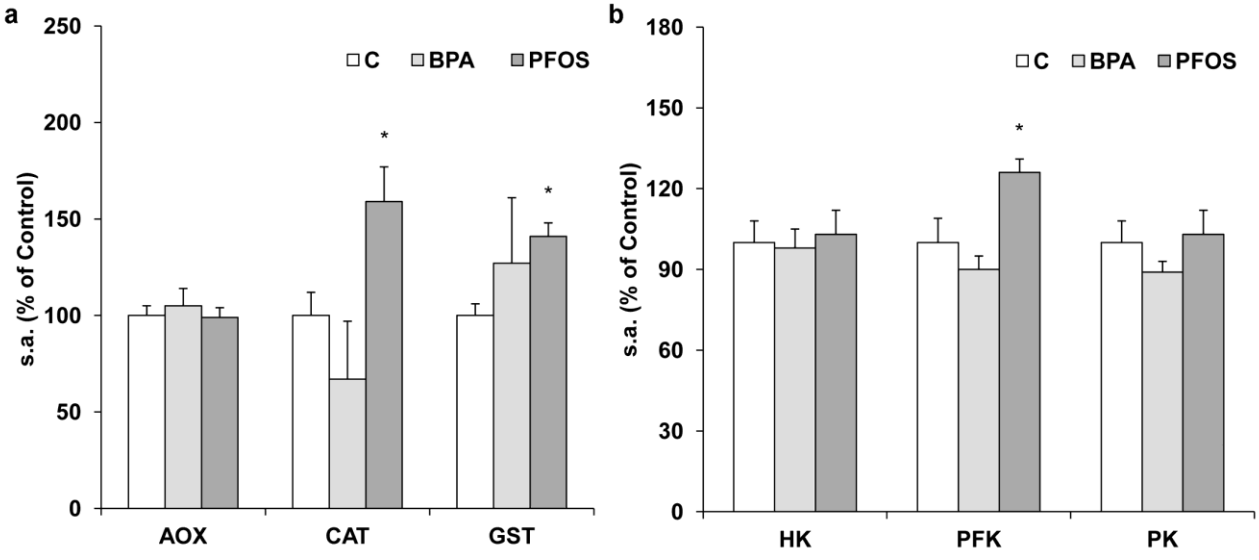

**Fig. 6**

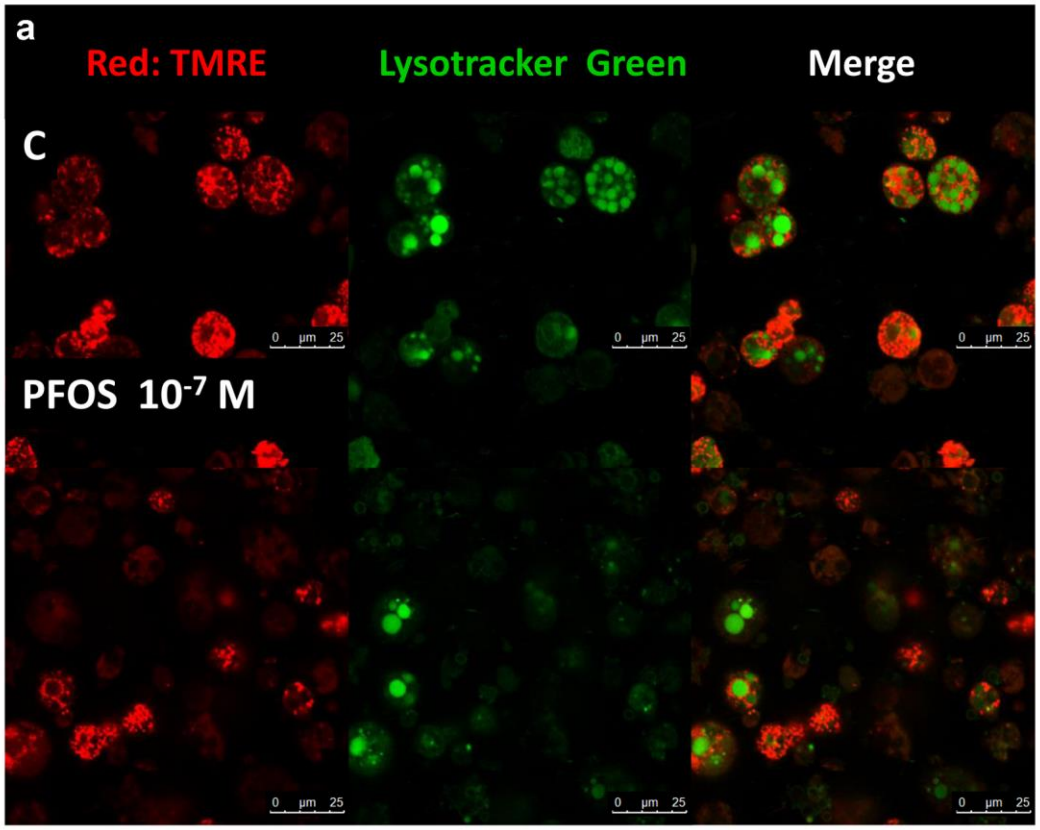
a
Red: TMRE
Lysotracker Green
Merge
C
PFOS 10-7 M
0 µm 25

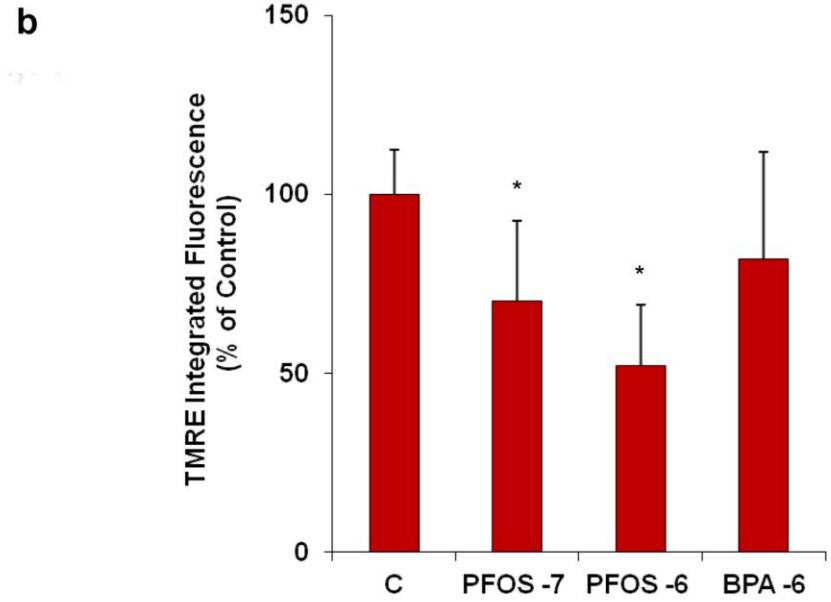
b
TMRE Integrated Fluorescence (% of Control)
150
100
50
0
*
*
C
PFOS -7
PFOS -6
BPA -6

**Fig.7**

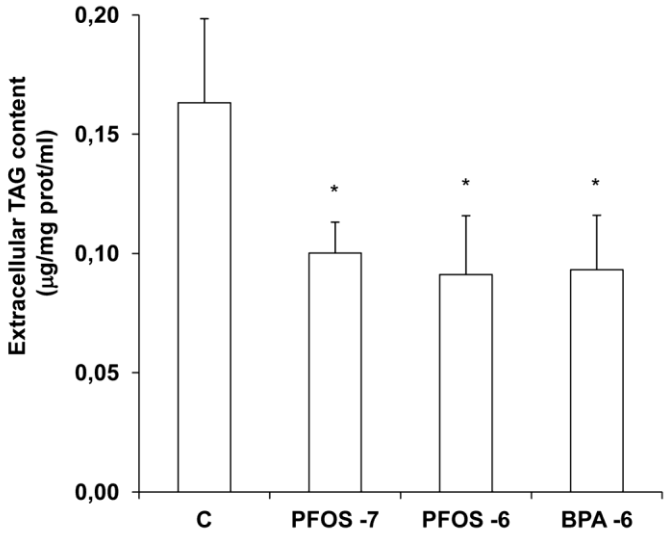
Extracellular TAG content (µg/mg prot/ml)
0,20
0,15
0,10
0,05
0,00
*
*
*
C
PFOS -7
PFOS -6
BPA -6

**Fig. 8**

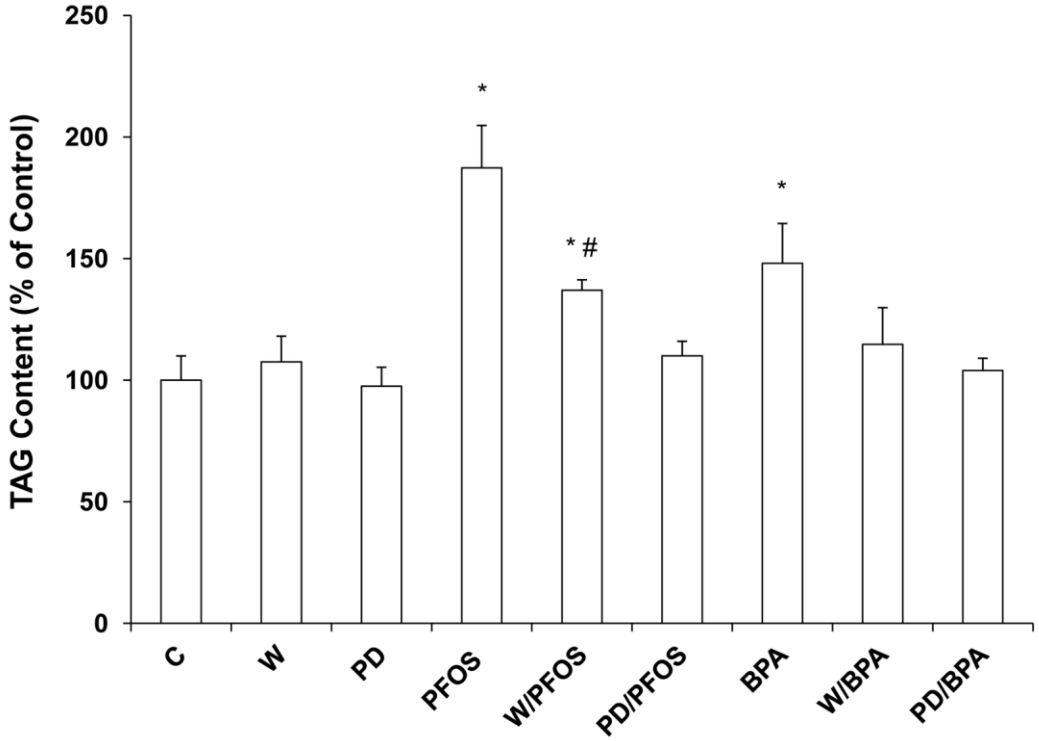
TAG Content (% of Control)
250
200
150
100
50
0
*
*#
*
C
W
PD
PFOS
W/PFOS
PD/PFOS
BPA
W/BPA
PD/BPA

**Table 1 - Functional and biochemical parameters in primary cultures of mussel digestive gland cells**.

Data represent the mean±SD values obtained by averaging the results obtained at 24 and 48 h post-isolation from 4 different cell preparations (n=8). LMS = Lysosomal membrane stability; AOX= Acyl-coA Oxidase; HK = hexokinase; PKF = Phosphofructokinase; PK= Pyruvate kinase; CAT = Catalase; GST = Glutathione transferase; TAGs = intracellular triglycerides

| | |
|---|---|
| LMS (NRRT, min) | 145±15 |
| AOX nmol/min/prot | 3.39±0.03 |
| HK nmoles/mg protein | 0.77±0.05 |
| PFK nmoles/mg protein | 3.25± 0.6 |
| PK nmoles/mg protein | 41±0.35 |
| CAT μmol/min/mg protein | 50.9±3.1 |
| GST nmol/min/mg protein | 171 ±12 |
| TAGs μg/mg prot/ml | 0.07±0.017 |

**Supplementary File 1**

*Analytical determination of organic chemicals in exposure medium*

Determination of organic chemicals by LC/MS was carried out as previously described (Achene et al. 2011): each chemical was suitably diluted from stock solutions in culture medium to obtain the desired final concentrations. Samples were extracted via solid-phase extraction (SPE), using Supelco HLB cartridges (glass 200 mg/6 cc, 60 µm) and analyzed by LC/MS/MS. Samples were acidified (HCl, pH 2) and spiked with internal standards (β-estradiol d3) before extraction under vacuum. The cartridges were conditioned with 3 mL of methanol and 3 mL of water and subsequently dried for 30 min by application of a gentle vacuum. The analytes were eluted with 6 mL of a mixture of Methanol:Acetone:Ethyl acetate (2:2:1 v/v/v) and concentrated to 100 µl using a nitrogen stream evaporator. The sample was reconstituted to a volume of 1 ml with a solution of water and methanol (1:1 v/v) and directly analyzed by a HPLC/MS/MS Varian system (Varian HPLC 212LC) coupled to 500 LC mass spectrometer using a C18 column (Ascentis Express, 15mm x 2.1mm x 2.7µm), mobile phase: 5 mM ammonium acetate/methanol in water. Procedural blanks were performed to ensure the absence of laboratory-contamination. Recoveries and reproducibility were determined using spiked water samples at a nominal concentration of 0.1 µg/l for each compound. For all chemicals, a linear response in the 0.005-1 µg/L range was obtained. Data obtained in samples at the concentration of 0.1 µg/L are summarized.

**Measured concentrations of organic chemicals in exposure medium (0.1 µg /L) as determined by SPE-HPLC/MS/MS.**

| | LOD ng/L | Exposure medium µg/L |
|---|---|---|
| BPA | 0.60 | 0.075 |
| TBBPA | 0.50 | 0.080 |
| PFOS | 0.06 | 0.085 |

**References**

Achene L., Bogialli, S., Lucentini, L., Pettine, P., Ottaviani, M. Eds. , 2011. Endocrine disruptors in Italy in water for human consumption. Report ISTISAN 11/18, 84 pp. (Istituto Superiore di Sanità, Italian National Health Institution) www.iss.it.

**Supplementary File 2**

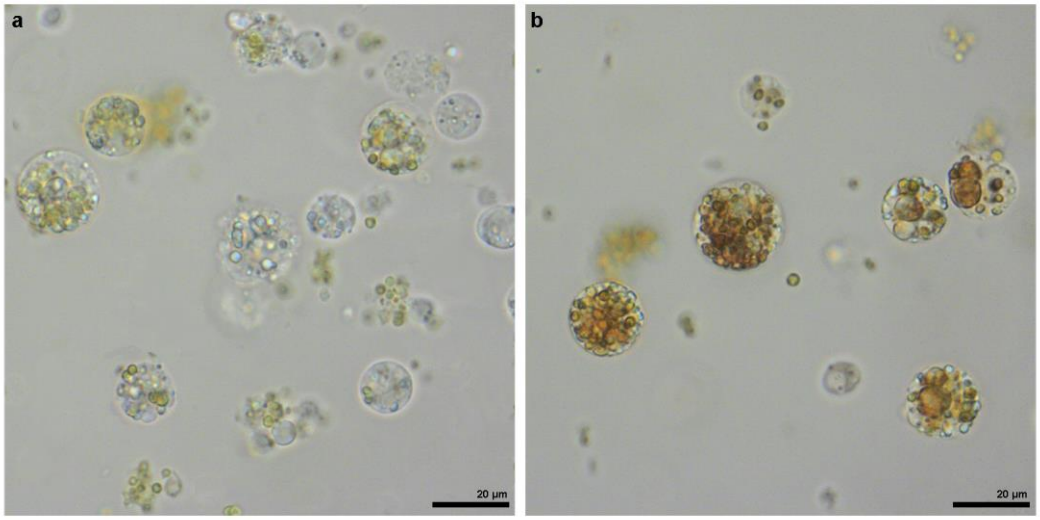

**Supplementary File 3**